Revealing “flickering” of the interaction strength in pA collisions at the CERN LHC

M. Alvioli, L. Frankfurt, V. Guzey, and M. Strikman

Phys. Rev. C **90**, 034914 — Published 29 September 2014

DOI: 10.1103/PhysRevC.90.034914

Revealing flickering of the interaction strength in pA collisions at the LHC

M. Alvioli

Consiglio Nazionale delle Ricerche, Istituto di Ricerca per la Protezione Idrogeologica, via Madonna Alta 126, I-06128 Perugia, Italy

L. Frankfurt

Tel Aviv University, Tel Aviv, Israel

V. Guzey

Petersburg Nuclear Physics Institute, National Research Center "Kurchatov Institute", Gatchina, 188330, Russia

M. Strikman

104 Davey Lab, The Pennsylvania State University, University Park, PA 16803, USA

Abstract

Using the high-energy color fluctuation formalism to include inelastic diffractive processes and taking into account the collision geometry and short-range nucleon–nucleon correlations in nuclei, we assess various manifestations of flickering of the parton wave function of a rapid proton in pA interactions at LHC energies in soft QCD processes and in the special soft QCD processes accompanying hard processes. We evaluate the number of wounded nucleons, N_{coll} — the number of inelastic collisions of projectile, in these processes and find a nontrivial relation between the hard collision rate and centrality. We study the distribution over N_{coll} for a hard trigger selecting configurations in the nucleon with the strength larger/smaller than the average one and argue that the pattern observed in the LHC pA measurements by CMS and ATLAS for jets carrying a large fraction of the proton momentum, x_p, is consistent with the expectation that these configurations interact with the strength which is significantly smaller than the average one — a factor of two smaller for $x_p \sim 0.5$. We also study the leading twist shadowing and the EMC effects for superdense nuclear matter configurations probed in the events with a larger than average number of wounded nucleons. We also argue that taking into account energy–momentum conservation does not change the distribution over N_{coll} but suppresses hadron production at central rapidities.

I. INTRODUCTION

Recently a very successful proton–lead run has been performed at the LHC which employed several detectors with the acceptance of many units in rapidity. It was observed in [1] that interpretation of pA data depends significantly on whether one uses as the input model for pA interactions the Glauber model, which does not take into account fluctuations of the interaction strength, or the color fluctuation (CF) approach of [2, 3] and that it is difficult to describe the data without including such fluctuations. The color fluctuation formalism takes into account the space–time evolution characteristic for the interaction of composite states in high energy processes in QED and QCD. In particular, the Lorentz slowing down of interaction implies that an ultrarelativistic composite projectile interacts with a target through configurations of partons whose characteristic lifetime (the coherence length) becomes large at high energies and whose interaction strengths with the target, σ, may significantly vary. The fact that the projectile can exist in the frozen fluctuations/configurations of partons with different interaction cross sections is called "flickering" in our paper.

Small-size parton configurations with small σ in a meson wave function were observed in fixed-target data on pion–nucleus collisions at FNAL and in electron–nucleus scattering at TJNAF (for a recent review, see [4]). Fluctuations to "large" nucleon configurations with the larger than average σ are an unambiguous consequence of the CF approach [2]. Their contribution allows one to explain the significant large-N_{coll} tail in the distribution over the number of inelastic collisions, N_{coll}, indicated by the ATLAS data [1].

The aim of this paper is to analyze how fluctuations of the interaction strength, the momentum conservation, the composite structure of hadrons, parton–parton correlations in the parton wave function of a fast projectile hadron and presence of the superdense nuclear matter configurations reveal themselves in the structure of final states in pA collisions at the LHC energies.

The paper is organized as follows. In Sect. II we explain that the large coherence length for the interaction of fast nucleons (which is comparable at the LHC energies to the radius of an atom) results in the necessity to take into account the significant cross section of diffractive processes in proton–nucleon (pN) collisions. For proton–deuteron (pd) collisions, this leads to the Gribov–Glauber model of nuclear shadowing for the total pd cross section [5]. Employing completeness over diffractively produced states allows one to include effects of inelastic diffraction in the interaction of projectile with any target. This approximation leads to the CF approach, which provides a constructive method to calculate the interaction of projectile with any number of target nucleons.

In addition, we explain how to include well understood properties of bound states in QCD into the formulae of the CF approach. We review the basic formalism and present predictions for the distribution over the number of inelastically interacting nucleons, N_{coll}.

In Sect. III we evaluate fluctuations of N_{coll} due to CF phenomena in soft QCD processes accompanying a hard trigger. The developed formalism explicitly satisfies the QCD factorization theorem for hard inclusive processes and allows us to evaluate the rate of hard processes as a function of the number of wounded nucleons N_{coll} taking accurately into account the difference of the impact parameter geometry of hard and soft collisions. Significant deviations from the often assumed linear dependence of the hard rate on N_{coll} are observed.

In Sect. IV we discuss several strategies for observing effects of proton flickering in pA collisions with a hard trigger. In particular, we argue that such studies would allow one to determine the correlation between the x distribution of partons in the nucleon and the overall interaction strength and, in particular, to test the hypothesis that the proton size is shrinking with an increase of x. We compare distributions over N_{coll} for triggers corresponding to the larger/smaller than average interaction strength. In particular, we find an enhancement of the jet rate for the peripheral collisions in which x of the proton is large enough so that smaller than average configurations in the proton are selected. We discuss a connection of our results to the recent measurements at the LHC using two large acceptance detectors (ATLAS and CMS), which studied the dependence of jet production as a function of the centrality, which was defined via the measurement of the transverse energy distribution in the nuclear fragmentation region. We argue that the pattern observed for the forward jet production (along the proton direction) matches that for the interaction of the proton CF with the strength, which is approximately a factor of two smaller than on average.

In Sect. V we consider effects of perturbative QCD (pQCD) evolution on color fluctuations for fixed-x configurations in the nucleon. We evaluate the range of x at the low Q scale contributing to the strength of fluctuations for the same x at the hard probe scale of the order of 100 GeV.

In Sect. VI we consider effects due to deviation of nuclear parton distribution functions (PDFs) from the sum of nucleon PDFs which were neglected in the previous sections since they are small in the currently studied kinematics. We focus on the limit when a trigger may select collisions where the number of wounded nucleons exceeds significantly the average number of nucleons at small impact parameters, which—due to the significantly higher local density—corresponds to selection of configurations in the nucleus wave function for which the parton distribution is different from the average one. We demonstrate that for these collisions, both nuclear shadowing and the EMC effect are significantly enhanced, with the EMC effect probing local nucleon densities comparable

to those in the cores of neutron stars.

In the Appendix we explain how to implement energy–momentum conservation according to general principles of QCD and show that the formulae of the Gribov–Glauber model and the CF approach for the total cross section and the number of wound nucleons are not modified. At the same time, the formulae for the double hadron multiplicity in pd collisions (as well as for triple and higher multiplicities in pA scattering) are modified by a model-dependent factor due to an increase of the inclusive cross section with energy. This leads to violation of the Abramovski–Gribov–Kancheli (AGK) cutting rules [6] for the inclusive hadron cross section.

II. COLOR FLUCTUATIONS FORMALISM FOR HADRON–NUCLEUS COLLISIONS AT HIGH ENERGIES

In this section we summarize the framework for the quantitative description of flickering phenomena in high energy processes which we refer to as the color fluctuation (CF) approach. This framework allows one to take into account the contribution of the diffractive excitation of a projectile proton and implement well-understood QCD properties of hadrons and their interactions. One of such properties is presence of the significant fluctuations of the interaction strength, for a more detailed discussion, see [7]. Several types of fluctuations are known at present: fluctuations of the sizes and the shapes of the colliding hadrons, of number of interacting constituents, etc. Following our previous papers we will refer to all these fluctuations as color fluctuations. In the physics of fluctuation phenomena, a significant part of fluctuation effects can be evaluated in terms of the dispersion of the interaction strengths which is calculable in terms of the cross section of inelastic diffractive processes in pN scattering, see Eq. (3) below.

It has been understood long ago that in the case of high energy processes, the contribution of the planar Feynman diagrams relevant for the Glauber approximation in non-relativistic quantum mechanics is zero and that the dominant contribution arises from non-planar diagrams [8, 9]. Gribov suggested [5] to rewrite the sum of non-planar diagrams as the sum over diffractively produced hadronic intermediate states.

The Gribov–Glauber model has been further generalized to take into account effects of the compositeness of a projectile hadron in inelastic interactions with nuclei [2]. This generalization is justified because at high energies it is possible to neglect effects of $t_{min} \neq 0$ (t_{min} is the minimal kinematically allowed four-momentum transfer squared) in the production of diffractive excitations of the projectile and, hence, to sum over produced diffractive states using the condition of com-

pleteness: $\sum_n |n\rangle \langle n| = I$, where I is a unit matrix. The requirement of small $-t_{min} \leq 3/R_A^2$ puts a limit on the masses of the intermediate states, M_{diff}, which in the case of nuclei corresponds to

$$M_{diff}^2/s < \sqrt{3}/R_A m_N \,, \tag{1}$$

or, equivalently, to the configurations in the projectile proton frozen over the coherent length l_c:

$$l_{coh} = \frac{s}{m_N(M_{diff}^2 - m_N^2)} \gg 2R_A \,, \tag{2}$$

where m_N is the nucleon mass; R_A is the nucleus radius; s is the square of the center-of-mass energy.

The first step in the derivation of CF formulae is to notice that the strength of the interaction with n nucleons is modified as compared to the Glauber model by the factor of $\lambda_n \equiv \langle \sigma^n \rangle / \sigma_{tot}^n$ which sums contributions of all diffractive intermediate states. The factors of λ_n can be expressed in terms of the distribution over cross sections $P_N(\sigma)$, $\lambda_n = \int_0^\infty d\sigma (\sigma/\sigma_{tot})^n P_N(\sigma)$, where $P_N(\sigma)$ is the probability for a proton to interact with the target with the given cross section σ and $\sigma_{tot} = \int_0^\infty d\sigma \sigma P_N(\sigma)$ is the total proton–nucleon cross section. The distribution $P_N(\sigma)$ depends on the incident energy, which will be discussed later.

By construction, $\lambda_0 = \lambda_1 = 1$ due to the probability conservation and the definition of the total cross section. The variance of the distribution $P_N(\sigma)$ is

$$\lambda_2 - 1 = \int_0^\infty d\sigma \, P_N(\sigma) \left(\frac{\sigma}{\sigma_{tot}} - 1 \right)^2 \equiv \omega_\sigma = \left. \frac{\frac{d\sigma(p+p\to X+p)}{dt}}{\frac{d\sigma(p+p\to p+p)}{dt}} \right|_{t=0} , \tag{3}$$

where the sum over diffractively produced states X is implied. Equation (3) follows directly from the optical theorem and the definition of $P_N(\sigma)$. It was derived originally in [10] within the approach of [11]. The analysis of the fixed target data [12] indicates that the variance ω_σ first grows with energy reaching $\omega_\sigma \sim 0.3$ for $\sqrt{s} \sim 100$ GeV and then starts to decrease at higher energies dropping to $\omega_\sigma \sim 0.1$ at the LHC energies.

Thus in contrast to the case of lower energies, the cross section is calculable in terms of scattering of frozen parton configurations in the wave function of a rapid projectile and then summing over contributions of these configurations. In the case of averaging of quantities depending on one variable σ, we may introduce the following unit matrix, $\int d\sigma \delta(\sigma - \sigma(x_i, \rho_{i,t}))$, where x_i and $\rho_{i,t}$ are the light-cone fractions and transverse coordinates of the partons, integrate over all variables characterizing the wave function of the projectile, ψ, and obtain:

$$\int |\psi(x_i, \rho_{i,t})|^2 \delta(\sigma - \sigma(x_i, \rho_{i,t})) d\tau = P_N(\sigma) \,, \tag{4}$$

where $d\tau$ is the phase volume. This formula indicates that selection of certain parton configuration in the projectile may influence the effective value of σ. Note also that the contribution of large diffractive masses described by triple Pomeron processes is restricted by the kinematics $M^2_{diff}/s \ll 1/m_N R_A$. Thus, at large s, participating parton configurations within the projectile are frozen during collisions and the contribution of large diffractive masses can be included in Eq. (4). This means that the CF approach also includes large diffractive masses corresponding to triple Pomeron processes.

Important properties of $P_N(\sigma)$ follow from rather general reasoning:

(i) $P_N(\sigma)$ is positive and rapidly decreasing with an increase of σ to ensure finiteness of the moments $\int P_N(\sigma)\sigma^n d\sigma$.

(ii) $P_N(\sigma)$ is a continuous function of σ with $P_N(0) = P_N(\sigma \to \infty) = 0$, which follows from applicability of pQCD at $\sigma \to 0$, see the discussion below. Hence, $P_N(\sigma)$ should have a maximum at $\sigma = \sigma_0$ corresponding to an average configuration of partons in the nucleon, see Eq. (5) below. Thus, σ_0 is close to the observed total nucleon–nucleon (NN) cross section.

(iii) The distribution over σ around the average configuration is controlled by the variance ω_σ. The variance is expressed in terms of the cross section of inelastic diffraction at $t = 0$, see Eq. (3).

The data indicate that the variance first grows with energy reaching $\omega_\sigma \sim 0.3$ for $\sqrt{s} \sim 100$ GeV and then starts to decrease for higher energies. The current LHC data on diffractive processes in pp collisions are not sufficient to determine accurately ω_σ directly from the data. Still the data are consistent with the trend that the interaction at small impact parameters becomes practically black and hence does not lead to inelastic diffraction. Overall, extrapolations from the lower energies and an inspection of preliminary LHC data indicate that the ratio of diffractive and elastic cross sections at $t = 0$ drops with energy and that $\omega_\sigma(\sqrt{s} = 5 \text{ TeV}) \approx 0.1$. (This is close to the extrapolation of the pre-LHC data fit for ω_σ by K. Goulianos [13] to LHC energies.) Naively this looks like a small number but it corresponds to a rather broad distribution over σ. For example, modeling $P_N(\sigma)$ by introducing two diffractive states of equal probability, one would find that they should have the cross sections that differ by nearly a factor of two: $\sigma_i = \sigma_{tot}(1 \pm \sqrt{\omega_\sigma})$. This indicates that even at the LHC, the nucleon can interact with a significant probability both with the super large strength ~ 130 mb and the significantly smaller than average strength ~ 70 mb.

(iv) In the region of large σ one can use several generic considerations. Since the variance is small at the LHC energies, the distribution around the maximum is comparatively narrow and in practical calculations, the region of $\sigma \gg \sigma_0$ gives a negligible contribution. Thus, a reasonable approximation is take into account only small fluctuations around the average value of σ. Then, as

in the classical and quantum mechanical theory of small fluctuations around average value, $P_N(\sigma)$ in the vicinity of $\sigma = \sigma_0$ should have the form close to the Gaussian distribution in σ. Note also that models with different patterns of fluctuations such as, e.g., the model with two cross section eigenstates but the same ω_σ [3] and the model with $P_N \propto \exp[-c\,|\sigma - \sigma_0|\,/\sigma_0]$ lead to very similar numerical results.

(v) At small σ, $P_N(\sigma) \propto \sigma$ which follows from QCD quark models of the proton and approximate proportionality of the cross section of interaction of small-size $|3q\rangle$ configurations with target nucleons to the area occupied by color as follows from pQCD, see e.g.[14]. Under these assumptions, the derivation is effectively reduced to the application of QCD quark counting rules. Note that for a projectile meson, $P_\pi(\sigma) \propto const$ at $\sigma \to 0$ [12]. In perturbative QCD, the interaction cross section of small-size configurations is small but grows with energy faster than that of average-size configurations. As a result, $P_N(\sigma)$ is expected to decrease rather rapidly with s for fixed $\sigma \ll \sigma_0$.

A competing parametrization of $P_N(\sigma)$ based on the Poisson distribution has been suggested in [15] for RHIC energies. In this parametrization, $P_N(\sigma) \propto \sigma^{k-1}\exp(-\sigma/\theta)$, with $k = 1/\omega_\sigma$. For RHIC (LHC), where $\omega_\sigma \approx 0.25$ (0.1), this corresponds to $P_N(\sigma)_{|\sigma\to 0} \propto \sigma^3(\sigma^9)$, which is much faster than in the quark models where $P_N(\sigma)_{|\sigma\to 0} \propto \sigma$.

(vi) The resulting form of $P_N(\sigma)$ is a smooth interpolation between the small-σ and large-σ regimes. In our numerical studies we use results of the theoretical analysis of [12] which determined first three moments of $I_n = \int \sigma^n P_N(\sigma) d\sigma$ using the normalization condition for $P_N(\sigma)$, Eq. (3) for the variance and the data on coherent diffraction off the deuteron and implemented the small-σ behavior of $P_N(\sigma)$ expected in pQCD:

$$P_N(\sigma) \;=\; \gamma\,\frac{\sigma}{\sigma+\sigma_0}\exp\left\{-\frac{(\sigma/\sigma_0\;-\;1)^2}{\Omega^2}\right\}, \tag{5}$$

where $\Omega^2/2 \approx \omega_\sigma$ numerically. In the $\omega_\sigma \to 0$ limit, $\Omega^2 = 2\omega_\sigma$ and the parametrization of Eq. (5) converges to $\delta(\sigma - \sigma_{tot})$. The analysis [12] of the data on coherent diffraction off the deuteron at E_p= 400 GeV shows that this distribution is approximately symmetric around $\sigma = \sigma_{tot}$.

Equation (5) is qualitatively different from $P_N(\sigma)$ suggested in [10] to describe pN scattering using the pre-QCD idea that only wee partons are involved in the high energy hadron–hadron interaction. In particular, instead of the behavior $P(\sigma \to 0) \propto \sigma$, the authors of [10] suggested that $P_N(\sigma \to 0) \propto \delta(\sigma)$.

For pA collisions at $\sqrt{s}$=5.02 TeV studied at the LHC, we use σ_{tot} = 93 mb and ω_σ = 0.1 leading to γ = 0.0263914, σ_0 = 86.4825 mb, and Ω = 0.51285. Although experimentally the value of $\omega_\sigma = 0.1$ appears to be preferred for the energies probed in pA collisions at the LHC, in

several cases we will illustrate sensitivity to the value of ω_σ by presenting numerical results also for $\omega_\sigma = 0.2$.

To evaluate the cross sections of the events where the number of collisions is exactly N_{coll}, where N_{coll} is the number of target nucleons involved in the inelastic interaction with the projectile, one needs the distribution over inelastic cross sections, $P_{inel}(\sigma_{inel})$. This distribution is calculable in terms of $P_N(\sigma)$ since all above discussed restrictions on $P_{inel}(\sigma_{inel})$ and $P_N(\sigma)$ are the same except for the normalization. Moreover, since experimentally the fraction $1-\lambda$ of the total cross section due to elastic scattering is a rather weak function of the incident energy, it is natural to assume that this is also true for each individual proton fluctuation. Thus, the variances of $P_{inel}(\sigma_{inel})$ and $P_N(\sigma)$ are equal and one can restore $P_{inel}(\sigma_{inel})$ using the following relation:

$$P_{inel}(\sigma_{inel} = \sigma\frac{\sigma_{inel}}{\sigma_{tot}}) = \frac{\sigma_{inel}}{\sigma_{tot}} P_N(\sigma)\,. \tag{6}$$

In the discussed approximation one can rewrite $\sigma_{in}(pA)$ as a sum of positive cross sections of inelastic interactions with exactly N_{coll} nucleons analogously to the case of the Gribov–Glauber approximation of [16]. A compact expression for $\sigma_{in}(pA)$ can be written, if internucleon correlations in the nucleus and the finite radius of the NN interaction are neglected:

$$\begin{aligned}
\sigma_{in}^{hA} &= \sum_{N_{coll}=1}^{A} \sigma_{N_{coll}}\,, \\
\sigma_{N_{coll}} &= \int d\sigma P_{inel}(\sigma) \frac{A!}{(A-N_{coll})!\,N_{coll}!} \int d^2\boldsymbol{b}\, x(b)^{N_{coll}} \left[1-x(b)\right]^{A-N_{coll}}\,,
\end{aligned} \tag{7}$$

where $x(b) = \sigma T(b)/A$ and the normalization is $\int d^2\boldsymbol{b}\, T(b) = A$. This formula is a generalization of the optical approximation to the relativistic domain where inelastic processes give the dominant contribution to the total cross section. In the framework of the Gribov Reggeon calculus, the factor of $x(b)^{N_{coll}}$ corresponds to N_{coll} cut Pomeron exchanges and the factor of $[1-x(b)]^{A-N_{coll}}$ — to $A-N_{coll}$ uncut Pomeron exchanges.

It is straightforward to include the effect of the finite radius of the NN interaction as the probability for two nucleons to interact inelastically while at a relative impact parameter b_{12}, $P(b_{12})$. It is expressed through the profile function of NN scattering, $\Gamma(b_{12})$, as $P(b_{12}) = 1-|1-\Gamma(b_{12})|^2$. The resulting formula (an analogue of Eq. (25) of [16] written in the approximation when correlations between nucleons are neglected) is essentially probabilistic reflecting the semiclassical picture of high energy inelastic interactions with nuclei. The Monte Carlo (MC) which includes accurately both geometry of the NN interactions and nuclear correlations was presented in [3]. It is used in our numerical studies described below.

Hence the probability of inelastic collisions with exactly N_{coll} nucleons, $P_{N_{coll}}$, is simply:

$$P_{N_{coll}} = \sigma_{N_{coll}}/\sigma_{in}^{hA} \,. \tag{8}$$

For the average number of collisions, one finds

$$\langle N_{coll} \rangle = \sum_{N_{coll}=1}^{A} N_{coll}\sigma_{N_{coll}}/\sigma_{in}^{hA} = A\sigma_{in}/\sigma_{in}^{hA} \,, \tag{9}$$

which depends very weakly on ω_σ [3] since the inelastic shadowing correction to σ_{in}^{hA} is very small because the pA interaction is nearly black at the LHC energies.

In terms of non-planar diagrams, energy–momentum conservation is automatically fulfilled. This implies that taking into account energy–momentum conservation does not produce additional factors in the formulae of the Gribov–Glauber and CF approaches for the total cross sections, inelastic shadowing and hadron multiplicities at the rapidities close to the nucleus fragmentation regions. In contrast, the formulae for the double, triple, etc. hadron multiplicities contain additional suppression factors to satisfy energy–momentum conservation, see the discussion in the Appendix.

In the approximation of [16], σ_{inel} did not include inelastic final states with the nucleus breakup but without hadron production. Correspondingly, in our case, when a particular configuration can scatter elastically off a nucleon of the nucleus, the final states corresponding to the excitation of the projectile without hadron production of the nucleus fragmentation are not included in σ_{inel} in Eq. (7) (or its finite radius of interaction version). Namely, Eq. (7) does not include the cross section of coherent inelastic diffraction, which is less than 1% of the total inelastic cross section [17], and quasielastic scattering with the nucleus breakup. Incoherent diffraction is dominated by scattering off the nucleus edge which is roughy equal to the product of the probability of the interaction with one nucleon ($\sim$ 20%, see Fig. 1) and the probability of single diffraction for a given proton in inelastic pp collisions, which is $\sim 10 - 15\%$, leading to the overall probability of incoherent diffraction of $\sim 2 - 3\%$.

These contributions are also not included in the LHC pPb events samples – events without rapidity gaps. This allows one to exclude the Coulomb excitation contribution which may reach 10% of the inelastic cross section [17]. This cut removes from the sample also most of the rapidity gap events due to the inelastic diffraction dissociation of the proton and the nucleus. A type of the events which is included in our definition of σ_{inel} but not in the experimental definition is quasielastic scattering in which nucleon (nucleons) of the nucleus are diffractively excited. In principle one needs to include this correction in the comparison of the calculations with the data, although as we have seen above, in most of the cases it is a very small effect.

The finite radius of the nucleon–nucleon interactions and short-range NN correlation effects were implemented in the Monte Carlo procedure of Ref. [3]. The algorithm generates multi-nucleon configurations in nuclei with correct short-range correlations of protons and neutrons developed in [18] and uses the profile function for the dependence of the probability of inelastic NN collisions on the relative impact parameter as given by the Fourier transform of the elastic pp amplitude and S-channel unitarity. Fluctuations of the interaction strength are included by assigning incoming protons the values of σ with the measure given by $P_N(\sigma)$.

In Ref. [3] a detailed comparison of the predictions for the number of wounded nucleons with and without taking into account color fluctuations was presented. It was demonstrated that the inclusion of fluctuations leads to a significant change of the distribution over the number of wounded nucleons both for a fixed impact parameter and for the integral over impact parameters. A large enhancement of the probability of the events with large N_{coll} was observed (see Fig. 1).

As usual for the random phenomena, in a wide range of N_{coll}, the probability distribution over N_{coll} ($P(N_{coll})$) is most sensitive to the value of the variance ω_σ. In particular, the parametrization of Eq. (5) and the two-state model were found to give very close results in a wide range of N_{coll}.

The results of our numerical studies using the Glauber model (corresponding to $\omega_\sigma = 0$) and the CF model with two values of ω_σ ($\omega_\sigma = 0.1$ and 0.2) are presented in Fig. 1. The calculation is done using the Monte Carlo algorithm developed by two of the present authors and described previously [3]. The profile function was also scaled with σ to satisfy the condition that the interaction is black at small impact parameters. One can see from the inset of Fig. 1 that our analysis demonstrates that the distribution over N_{coll} is sensitive to the value of ω_σ and that fluctuations result in the substantially larger tail of the distribution at large N_{coll}.

In Fig. 1 we showed the results of calculations based on the parametrization suggested in [12], which assumes the Gaussian shape of the large-σ tail of $P_N(\sigma)$. However, since the study [12] was testing fluctuations near its average value, σ_{tot}, it is reasonable to consider other options for large-σ asymptotic of $P_N(\sigma)$ in the present work. In particular, the tail of small-x parton distributions in the transverse plane is often fitted by the Gaussian distribution in ρ^2, where ρ is the parton transverse coordinate. If the cross section for large ρ is approximately proportional to the area, i.e., $\sigma \propto \pi\rho^2$, one would expect presence of the large-σ tail of $P(\sigma)$ that behaves as $P(\sigma) \propto \exp(-c\sigma)$. To probe sensitivity to the possible presence of such a tail, we introduce another model of $P_N(\sigma)$:

$$P_N(\sigma) = a\sigma \exp(-c\,|\sigma - \sigma_0|)\,, \tag{10}$$

with parameters fixed to reproduce the same total cross section and dispersion as in the basic

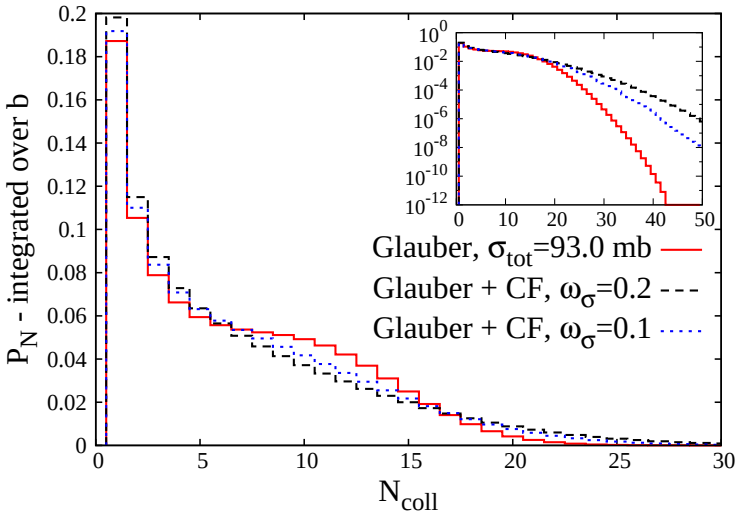

FIG. 1: The probabilities P_N of having $N = N_{coll}$ wounded nucleons, averaged over the global impact parameter b, as a function of N_{coll} for the Glauber model ($\omega_\sigma = 0$) and in the CF model with $\omega_\sigma = 0.1$ (our base value used in the current analysis) and $\omega_\sigma = 0.2$. The inset is in the log scale.

model. We find that the distribution over N_{coll} practically does not change – see Fig. 2.

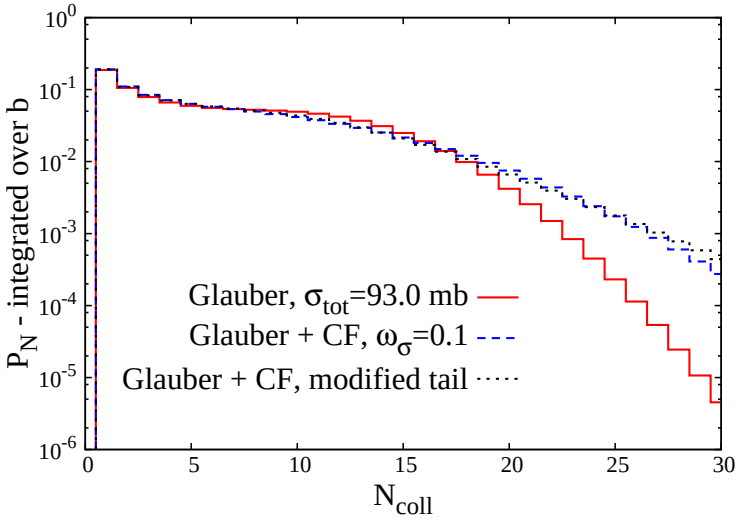

FIG. 2: Comparison of the distributions over $N = N_{coll}$ for the Glauber model and for the color fluctuation model with $\omega_\sigma = 0.1$ with the Gaussian [Eq. (5)] and exponential [Eq. (10)] large-σ behavior.

This confirms the conclusion of [3] based on the comparison of the model based on Eq. (5) and the two-component model. At the same time, changing the behavior at small σ one can generate a very different shape for the same variance, see Ref. [15]. Hence it would be interesting to explore this issue further as the sensitivity to the tail for central collisions should grow since at the LHC in central pA collisions, one typically selects $N_{coll} \sim 14$.

III. DISTRIBUTION OVER THE NUMBER OF COLLISIONS FOR PROCESSES WITH A HARD TRIGGER

We begin by addressing the long-standing question of the interplay of the phenomenon of color fluctuations and the partonic structure of the nucleon. It is well understood and observed experimentally that a hadron can exist in the configurations of different transverse sizes and that smaller configurations interact with a smaller cross section than the larger size configurations. This is one of the origins of flickering of the interaction strengths, which, as we mentioned in the Introduction, is present in both QCD and QED. Note here that a related phenomenon of fluctuations of the nucleon gluon density at fixed small x was inferred from exclusive hard processes in [19]. One of the typical setups for pA collisions is the study of soft phenomena which accompany a hard subprocess (dijet, Z-boson, ...) and is related to the number of wounded nucleons.

Our main aim is to get a deeper insight into dynamics of pA interactions and in particular to probe the flickering phenomenon which we discussed in the Introduction. In the case of inclusive production, the cross section is given by the QCD factorization theorem. An additional requirement on the final state breaks down the closure approximation and hence requires another form of the factorization theorem.

In this section we will consider nuclear PDFs as a sum of the nucleon PDFs since nuclear effects are small for large p_t studied at the LHC except possibly in the region of $x_A \geq 0.4$ where the EMC effect may play a role. Correspondingly we will use the impulse approximation to evaluate cross sections of hard process and the CF approach to calculate the number of wound nucleons accompanying the hard process. Effects related to the deviations of the nuclear PDFs from the additive sum of the nucleon PDFs—leading twist nuclear shadowing and the EMC effect—will be considered in Sect. VI.

On average, in the geometric model for hard processes in the kinematics, where nuclear shadowing can be neglected, i.e., for $x \geq 0.01$ and even smaller x for large virtualities, the multiplicity of events with a hard trigger (HT), which we will denote as $Mult_{pA}(HT)$, is $Mult_{pA}(HT) = \sigma_{pA}(HT+X)/\sigma_{pA}(in) = A\sigma_{pN}(HT+X)/\sigma_{pA}(in)$. Using $Mult_{pN}(HT) = \sigma_{pN}(HT+X)/\sigma_{pN}(in)$ and Eq. (9) (which to a very good approximation holds in the CF approximation [3]) one finds that a simple relation for the multiplicities of HT events in pN and minimal bias pA collisions holds:

$$Mult_{pA}(HT) = \langle N_{coll} \rangle \, Mult_{pN}(HT) \, . \tag{11}$$

Here we will consider the rates of hard collisions as a function of N_{coll} with the additional

factor of N_{coll} in the denominator in order to focus on the deviation from the naive optical model expectation [20] that Eq. (11) holds for fixed values of N_{coll}:

$$R_{HT}(N_{coll}) \equiv \frac{Mult_{pA}(HT)}{Mult_{pN}(HT)N_{coll}} = 1\,. \tag{12}$$

The impact parameter dependence of the cross section for the hard collision of two hadrons follows from QCD factorization theorem. It is given by the convolution of two generalized parton distributions which are functions of $\boldsymbol{\rho}_1$ and $\boldsymbol{\rho}_2$ – transverse distances of partons from the center of mass of the corresponding hadrons – with condition $\boldsymbol{\rho}_1 + \boldsymbol{b} - \boldsymbol{\rho}_2 = 0$ with accuracy $1/p_t(jet)$. When further integrating over $\boldsymbol{b}, \boldsymbol{\rho}_1, \boldsymbol{\rho}_2$ one obtains usual collinear expression for the cross section through the product of the pdfs of the hadrons, see e.g. discussion in [21].

To describe geometry of dijet production in proton – nucleus collisions let us introduce vectors $\boldsymbol{b}$ and $\boldsymbol{b_j}$ the transverse center of mass of the projectile proton and the target nucleons relative to the center of the nucleus, respectively. We also denote as $\boldsymbol{\rho}$ the transverse distance of the parton of the projectile from point $\boldsymbol{b}$. The transverse distance between the point of the hard collision and the distance to the transverse c.m. of nucleon j of the nucleus is

$$\boldsymbol{\rho}_j = \boldsymbol{b} + \boldsymbol{\rho} - \boldsymbol{b}_j\,. \tag{13}$$

The discussed geometry of collisions is shown in Fig. 3.

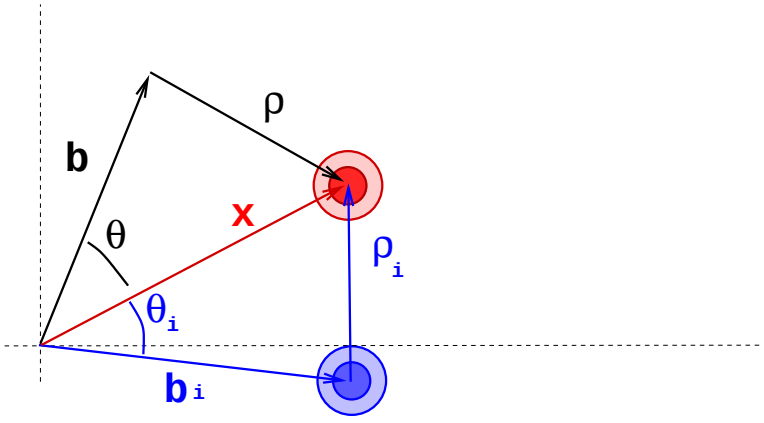

FIG. 3: Sketch of the transverse geometry of collisions.

The generalized gluon distribution in the nucleon can be parametrized as $g_N(x, Q^2, \rho) = g_N(x, Q^2)F_g(\rho)$, where $F_g(\rho)$ is the normalized distribution of gluons in the nucleon transverse plane (we do not write here explicitly the dependence of $F_g(\rho)$ on x and Q^2); $\int d^2\rho F_g(\rho) = 1$. This parametrization is reasonable since the distribution over ρ is practically independent on Q^2. In

our numerical calculations, we take $F_g(\rho)$ from the analysis of the data on elastic photoproduction of J/ψ mesons [21–23]. For $x \sim 0.01$:

$$F_g(b) = (\pi B^2)^{-1} \exp\left[-b^2/B^2\right], \tag{14}$$

where $B = 0.5$ fm. Note that sensitivity to the exact value of B is rather insignificant as long as x stays small enough.

The cross section differential in the impact parameter is given by convolution of the generalized gluon distributions of the colliding particles:

$$\frac{d\sigma_{HT}(NA)}{d^2b} = \sigma_{HT}(NN) \int d^2\rho \prod_{j=1}^{j=A} [d^2\rho_j] F_g(\rho) \times \sum_{j=1}^{j=A} F_g(\rho_j)\,, \tag{15}$$

where $\boldsymbol{\rho}_i$ is given by Eq. (13). The averaging over configurations in the nucleus is implied but not written explicitly.

It is worth emphasizing that Eq. (15) automatically corresponds to the impulse approximation for the total inclusive cross section of the HT process:

$$\int d^2b \frac{d\sigma_{HT}(NA)}{d^2b} = A\sigma_{HT}(NN)\,. \tag{16}$$

Up to this point, the integral over $d^2\rho$ can be performed analytically (or numerically) since the integrand function $F_g(\rho) \sum_{j=1}^{A} F_g(\mathbf{b} + \rho - \mathbf{b}_j)$, for a given configuration and given b, depends on ρ which has to take every possible value inside the nucleus.

However, the calculation of the distribution over N_{coll} involves taking into account that much smaller impact parameters dominate in hard collisions than in soft collisions [21, 23]. Also we want to be able to take into account correlations of nucleons in nuclei. Consequently the calculation can be performed only using a Monte Carlo technique.

The algorithm which leads to the impulse approximation expression for the cross section summed over the contributions of all N_{coll} is as follows.

(i) First a configuration of nucleons in the nucleus is generated and a particular value of b is chosen.

(ii) The quantity $F_g(\rho) \times \sum_{j=1}^{j=A} F_g(\rho_i)$ gives the weight of these configurations to the average when we calculate the integral over b.

(iii) The nucleon involved in the hard interaction is assigned to nucleon j with the probability given by

$$p_j = \frac{F_g(\mathbf{b} + \rho - \mathbf{b}_j)}{\sum_{k=1}^{A} F_g((\mathbf{b} + \rho - \mathbf{b}_k))}\,. \tag{17}$$

(iv) The number of other nucleons which interacted inelastically is calculated (that is, all nucleons except nucleon j); this number is $N_{coll}(other)$. This component of the procedure is identical to the one described for a generic calculation of N_{coll} without a trigger described in Sect. II. As a result, we can calculate now the probability that the interaction with the generated configuration will lead to N_{coll} active nucleons:

$$N_{coll} = N_{coll}(other) + 1\,, \tag{18}$$

and, hence, determine the probability that in the event there are exactly N_{coll}. We denote this probability as $p_{hard}(N_{coll}, event)$.

(v) Finally we calculate the rate of the hard collisions due to events with a specific number of collisions (we suppress here the overall factor of $\sigma_{pN}(HT)$):

$$\int d^2bd^2\rho \prod_{j=1}^{j=A}[d^2\rho_j]F_g(\rho) \times \sum_{j=1}^{j=A} F_g(\rho_i)p_{hard}(N_{coll}, event)\,. \tag{19}$$

The fraction of such events is simply

$$Frac(N_{coll}) = \frac{1}{A}\int d^2bd^2\rho \prod_{j=1}^{j=A}[d^2\rho_j]F_g(\rho) \times \sum_{j=1}^{j=A} F_g(\rho_i)p_{hard}(N_{coll}, event)\,. \tag{20}$$

As we explained above, in order to compare with the naive expectation of the Glauber model without correlations of any kind and the optical model limit, where one expects that the cross section of hard collisions for events with N_{coll} is $N_{coll}\sigma_{hard}(NN)$, we calculated the ratio given by Eq. (12). This procedure is obviously consistent with

$$\sum_{N_{coll}} \sigma(N_{coll})N_{coll} = A\sigma_{NN}\,. \tag{21}$$

Note here that in this discussion, we did not address the potential effect of energy–momentum conservation, see the Appendix.

First, we consider the case of average x_p for which there is no significant correlation between the value of σ for configuration and the parton distribution in the configuration. The case of x_p for which such correlations maybe present in considered in the next section. The results of our calculations are presented in Fig. 4 for $\omega_\sigma = 0$ (Glauber model) and for the CF model with $\omega_\sigma = 0.1$ (our base model) and $\omega_\sigma = 0.2$. Here we consider One can see that in the case of $\omega_\sigma = 0$, main deviations occur for small N_{coll} and the effect decreases with a decrease of σ_{tot}. It appears that the main reason for this deviation is that the transverse gluon distribution in the nucleus is narrower than the soft interaction profile function reflecting larger impact parameters in minimal bias NN

collisions than those in hard NN collisions [21, 23]. As a result, at large impact parameters (small N_{coll}) the probability of hard collisions decreases as compared to the naive expectations. With a decrease of $\sigma_{tot}(pp)$ and, hence, the b-range of NN interaction, the deviation of R_{HT} from unity is reduced.

This effect was first reported in [24] for AA collisions at RHIC and the LHC and for d-Au collisions at RHIC energies using the parameters of [21] for the impact parameter dependence of hard collisions and a simplified model for the impact parameter dependence of NN inelastic interactions.

Color fluctuations complicate the pattern of N_{coll}-dependence shown in Fig. 4 due to an additional effect of the broader distribution in b of the collisions with small σ (see Fig. 1 in [3]), which enhances the probability of collisions with small N_{coll} for small impact parameters, where the parton transverse density is higher. At very large N_{coll}, yet another new effect takes place, namely, fluctuations with large σ generate more collisions at large impact parameters, where the interaction is typically soft and does not lead to hard collisions. As a result, R_{HT} becomes smaller than unity, while in the model without fluctuations, R_{HT} stays very close to unity up to very large N_{coll}. We checked that results of our calculations are not sensitive to the presence of nucleon correlations in nuclei.

As a result, the CF approach predicts a higher rate of events with a hard trigger starting at somewhat larger N_{coll} than in minimum bias events (cf. Figs. 1 and 5). Hence our analysis demon-

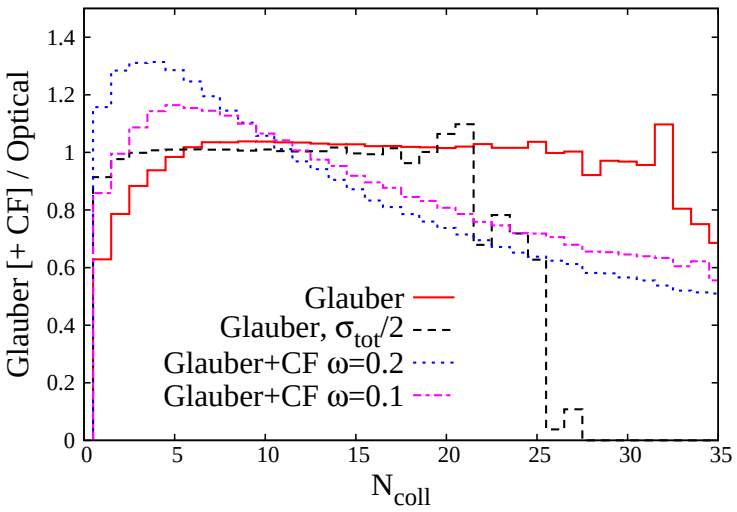

FIG. 4: Ratio R_{HT} (Eq. (12)) of the rates of hard collisions in the Glauber and the color fluctuation models to that in the optical model as a function of $N = N_{coll}$.

strates that color fluctuations lead to the following two effects for large N_{coll} for the bulk of hard

observables: (i) the larger probability of collisions with $N_{coll} \geq 12$ and (ii) the reduced probability of hard subprocesses for the same N_{coll} range. Further modeling is necessary to determine the optimal strategy to see these effects in the bulk data sample. Using the information on x_p of the parton in the proton undergoing the hard interaction may be an easier way forward.

IV. HOW TO OBSERVE THE EFFECTS OF FLICKERING IN pA COLLISIONS

In this section we propose strategies for using processes involving both soft and hard interactions to obtain the definitive evidence for the presence of the flickering phenomenon. The idea is to investigate the correlation between the light-cone fraction x_p of the parton in the proton involved in the hard collision and the overall interaction strength of the configuration containing this parton. The challenge for all such studies is that selection of certain classes of events (using a particular trigger) a priori post-selects different configurations in both colliding systems and these two effects have to be disentangled.

A natural question to ask is whether the parton distributions in configurations interacting with the strength smaller/larger than the average one are different and whether there exists a correlation between the presence of a parton with given x (and virtuality) and the interaction strength of this configuration. Naively one should expect presence of such correlations at least for large x. Indeed, if we consider configurations with large x, e.g., $x > 0.5$, one may expect that for such configurations the number of constituents should be smaller than on average (fewer $q\bar{q}$ pairs, etc.) as the consequence of the depletion of the phase volume for additional partons and selection of configuration with a minimal number of partons in the initial state before QCD evolution. Also, selection of x much larger than the average one should select larger than average longitudinal and transverse momenta in the nucleon rest frame, leading to a smaller than average size, see, e.g., [15, 20]. The shrinking may differ for large-x u and d quarks since the d/u ratio strongly depends on x for $x \geq 0.4$, see [25].

Let us consider pA collisions with a hard trigger which selects a parton with particular x in the proton projectile. As in the inclusive case, we use the distribution over the number of wounded nucleons as in Eq. (7) with the substitution $P(\sigma) \to P(\sigma, x)$. The distribution $P(\sigma, x)$ takes into account the probability for a configuration with given x to interact with the cross section σ. Due to the QCD evolution, $P(\sigma, x)$ also depends on the resolution scale (see Sect. V). Let us suppose that one can roughly measure the effective number of interacting nucleons within the nucleus, N_{coll}, based, e.g., on the energy release at the rapidities sufficiently far away from the central region (this

is the strategy adopted by ATLAS [26] and CMS [27]).

We demonstrated in the previous section that deviations of R_{HT} from unity are modest for fluctuations with $\sigma \leq \sigma_{tot}/2$. Neglecting deviations of R_{HT} from unity and nuclear modifications of PDFs (which is a small effect on the scale of the effects we consider here and which will be addressed later), we can use Eq. (7) to find the relation between $\langle\sigma(x)\rangle$ and experimental observables:

$$\frac{\left\langle\sigma^2(x)\right\rangle}{\sigma(x)} = \frac{(\langle N_{coll}\rangle - 1)\frac{A^2}{A-1}}{\int d^2bT^2(b)}\,. \tag{22}$$

Similarly, we can use Eq. (7) to determine higher order moments of $\sigma(x)$. For example, using Eq. (7) we find:

$$\frac{\left\langle\sigma^3(x)\right\rangle}{\sigma(x)} = \langle(N_{coll}-2)(N_{coll}-1)\rangle\,\frac{A^3}{(A-1)(A-2)\int d^2bT^3(b)}\,. \tag{23}$$

Hence by combining Eqs. (22) and (23) one can obtain information about the width of the distribution over $\sigma(x)$.

A more accurate calculation requires taking into account deviations from the $R_{HT} = 1$ approximation used above which may be significant for large N_{coll} (Sect. III). Such an analysis would require much more elaborate modeling of pA collisions.

Another strategy is possible which allows one to amplify the effect of flickering. We can consider the distribution over N_{coll} for N_{coll} much larger than $\langle N_{coll}\rangle$ for events with a hard trigger. In this case, scattering off small impact parameters dominates and fluctuations of σ are enhanced relative to the fluctuations of the impact parameter [39].

For the reasons described above, we expect the strongest modification of the distribution over the number of collisions for large enough x_p (this automatically requires large p_t >100 GeV/c for jets for the current acceptance of the LHC detectors, which allows one to safely neglect leading twist nuclear shadowing effects even if x_A is small).

To study the sensitivity of the number of wounded nucleons to the average $\sigma(x)$ for configurations selected by the trigger, we performed calculations with $\langle\sigma\rangle_x = \sigma_{tot}$, $\sigma_{tot}/2$ and $\sigma_{tot}/4$. Within the CF picture, the following two effects compete in generating large N_{coll} events: (i) selection of fluctuations in the nucleus wave function in which more nucleons happen to be at the impact parameter of the incoming proton (which, for large N_{coll} events, is anyway small $b < 3$ fm), and (ii) selection of fluctuations with $\sigma > \sigma(x)$. Our numerical studies show that there is large sensitivity to the mean value of $\sigma(x)$, even when we allow for significant fluctuations of $\sigma(x)$.

The results of these calculations are presented by the dashed curve in Fig. 5. One can see from the plot that for N_{coll} larger than the average number of collisions $\langle N_{coll}\rangle \approx 7$, in the minimal bias

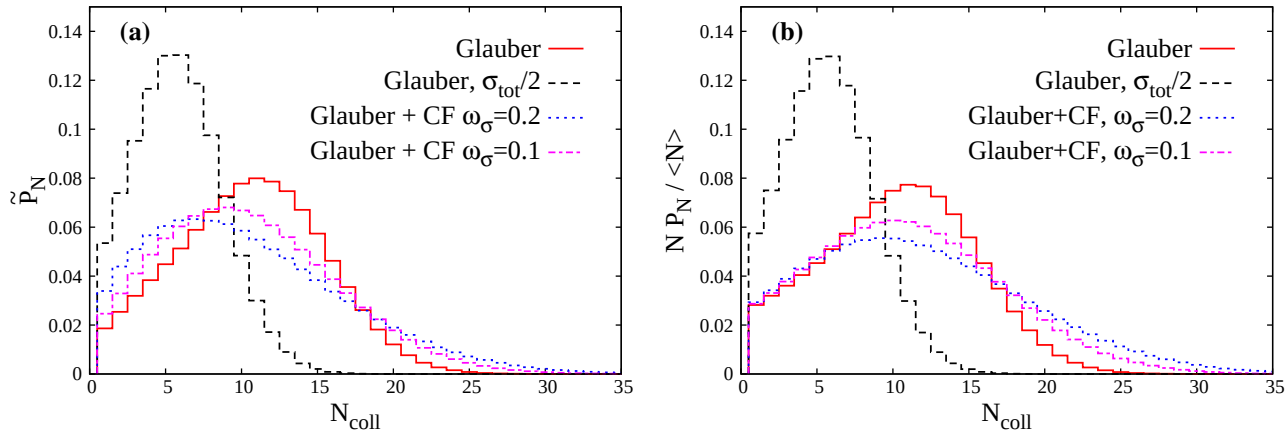

FIG. 5: The distribution over the number of collisions for a hard trigger using (a) the full calculation and (b) the approximation $R_{HT} = 1$.

events, one can easily observe the reduction of $\langle\sigma\rangle_x$ by a factor of two. To see whether flickering of the nucleon in the triggered configuration can mimic the change of $\langle\sigma\rangle_x$, we also considered the distributions for $\omega_\sigma = 0.1$ and 0.2, see the dotted and dot-dashed curves in the figure. One can see from the figure that this effect is not large enough to prevent the observation of reduction of $\langle\sigma\rangle_x$. The opposite limit is that of small enough x_p. In this case one would trigger on configurations with $\langle\sigma\rangle$ larger than the average one leading to broadening of the distribution over N_{coll}.

To illustrate the possible magnitude of the change in the x_A distribution as a function of N_{coll}, we present in Fig. 6 the ratios of $P_N(\sigma(x))/P_N(\sigma = \sigma_{in})$ for $\sigma(x)/\sigma_{in} = 2$, 1.5, 0.5, and 0.25 and $\omega_\sigma = 0$ and $\omega_\sigma = 0.1$ (for LHC energies) and $\omega_\sigma = 0.25$ (for RHIC energies) calculated using the procedure of Sect. III.

To illustrate the sensitivity to the pattern of flickering for fixed x, we use the scenario where $\langle\sigma(x)\rangle = \sigma_{tot}/2$ and proton fluctuations consist of two states with probabilities 2/3 and 1/3 with the respective cross sections $\sigma_{tot}/4$ and σ_{tot}. We compare the results of this model and the Gaussian-like model with the same variance equal 1/2 in Fig. 7. One can see that deviations from the results of the calculation with $\sigma = \sigma_{tot}$ are large in both cases . There is also significant difference in the high-N_{coll} tail.

Note in passing that the best way to check the difference between the transverse sizes of configurations with leading u- and d-quarks would be to measure leading W^+ and W^- production (one additional advantage is that in this case energy conservation effects would be the same for the two channels). Similarly, one can look for the difference in the accompanying multiplicity for forward $W^\pm$ production in pp scattering [32].

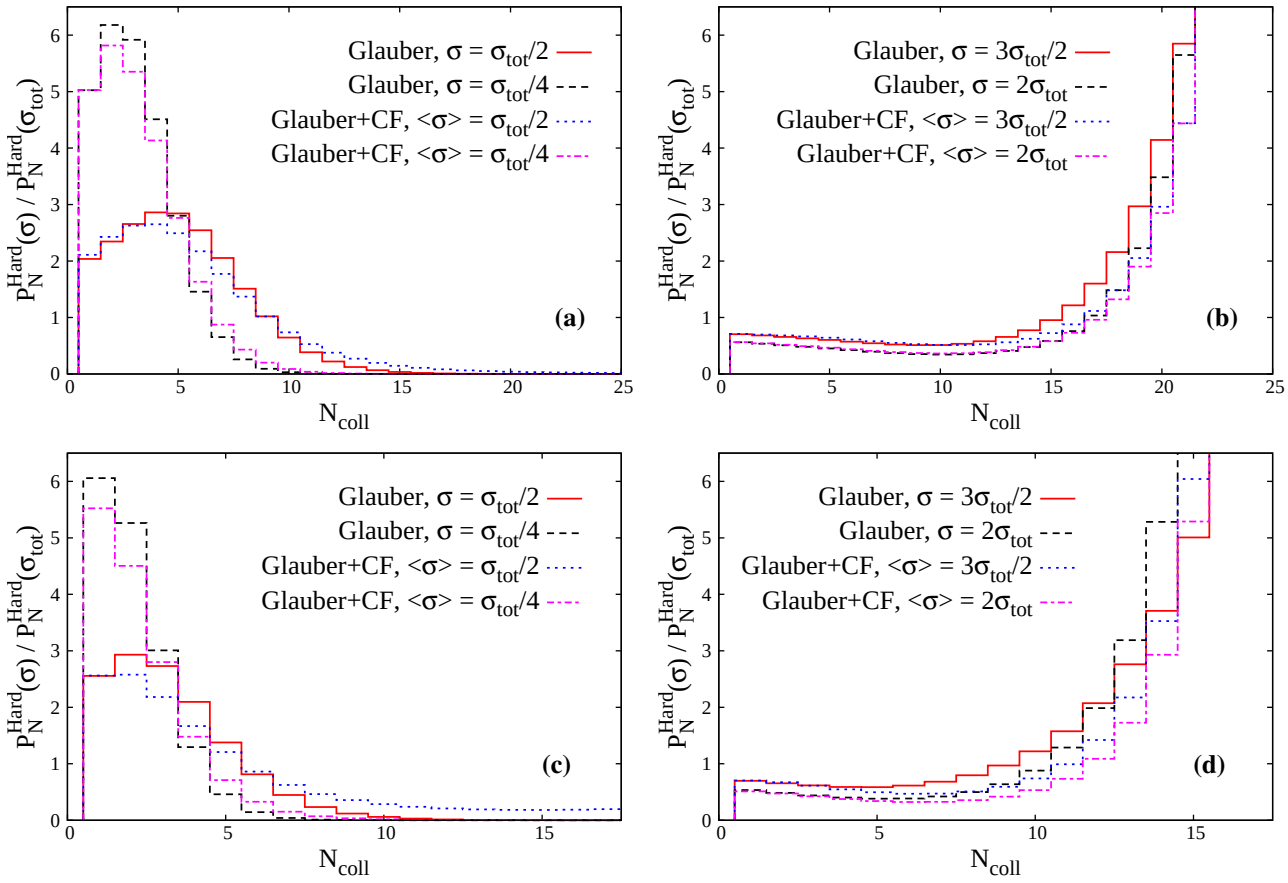

FIG. 6: Ratio of the probabilities P_N of having $N = N_{coll}$ wounded nucleons for configurations with different $\langle\sigma(x)\rangle$ and P_N for $\sigma = \sigma_{tot}$ at LHC (panels (a) and (b)) and RHIC (panels (c) and (d)) energies. The ratio is averaged over the global impact parameter b and plotted as a function of $N = N_{coll}$. The solid and dashed curves neglect the dispersion of σ, while the dotted and dot-dashed curves show the results obtained with a Gaussian distribution around $\langle\sigma(x)\rangle$ with the variance equal to 0.1. Panels (a) and (c) show results for NN interaction cross sections smaller than average, while panels (b) and (d) show results for NN interaction cross sections larger than average.

Overall an inspection of the numerical results presented in Figs. 5, 6, and 7 indicates that the selection of events with the highest nuclear activity—for example, the top 1%—greatly amplifies effects of flickering. Namely, the relative contribution of events with small σ is suppressed much stronger than in the events with smaller nuclear activity, leading to a strong distortion of the dijet distribution over x_p. Large-x_p rates (which are dominated by scattering off valence quarks of the proton) should be suppressed, while small-x rates, which are dominated by scattering off gluons, should be enhanced. A complementary way to study this effect is to consider the distribution over the energy deposited in the calorimeter as a function of x_p. We expect the monotonous shrinkage

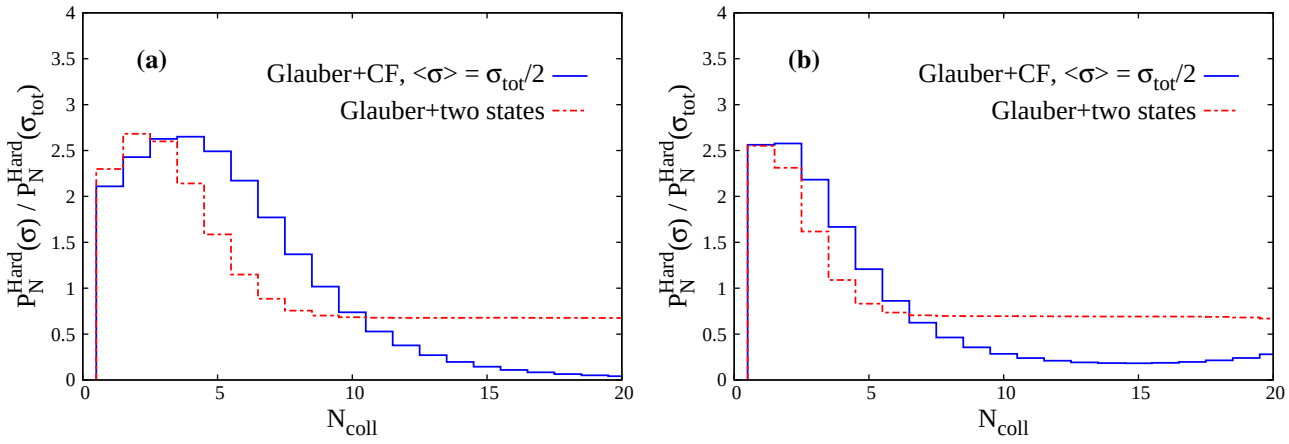

FIG. 7: Ratio of the probabilities P_N of having $N = N_{coll}$ wounded nucleons for configurations with different $\langle\sigma(x)\rangle$ and P_N for $\sigma = \sigma_{tot}$ for LHC (a) and RHIC (b) energies. The ratio is averaged over the global impact parameter b and plotted as a function of $N = N_{coll}$. The dashed curve is also shown in Fig. 6; see text for the definition of the two-state model shown by the dotted curve.

of the distribution over the number of collisions with increasing x, with the strongest effect for the highest number of collisions. Note in passing that such a study allows one to test the conjecture that large-x triggers select significantly smaller than the average-size configurations in the nucleon. Hence, such a study would allow one to rule out/confirm the explanation of the EMC effect as being due to the suppression of small-size configurations in bound nucleons [20].

The discussed patterns do not depend on details of the relation between N_{coll} and the signal in the calorimeter at negative rapidities (in the direction of the nucleus fragmentation). Qualitatively the discussed pattern is consistent with the pattern reported by ATLAS [26] and CMS [27]. Indeed, ATLAS observes the suppression of production of leading jets which they find to be predominantly a function of x_p, while the CMS analysis presents the correlation of the calorimeter activity with a different quantity $(\eta_{Jet_1} + \eta_{Jet_2})/2$ which still reflects the value of x_p [40].

In order to perform a detailed comparison of the CF model with the LHC data one needs data in bins of x_p. A preliminary version of such data was presented so far by ATLAS only. Also one needs a realistic model/models for the distribution over E_T for events with given N_{coll}. Such an analysis is underway and will be presented elsewhere. At the same time, we can obtain an estimate of the magnitude of the necessary change of average $\sigma(x \sim 0.5)$ using the data for most peripheral collisions (90%–60% centrality) where the expected enhancement is a rather weak function of N_{coll}. The data indicate an enhancement of the jet rate by a factor of about two. This corresponds to $\sigma(x \sim 0.5) \sim \sigma_{tot}/2$. It is worth emphasizing here that presence of an enhancement would be

difficult to understand based on the logic of energy losses.

V. PERTURBATIVE QCD EVOLUTION OF $P(\sigma, x)$

The distribution $P(\sigma, x)$ characterizes the distribution of strength of soft interactions of the configuration containing a parton carrying the light-cone fraction x at a sufficiently small resolution scale. A change of the scale—e.g., a change of p_T of the jets—does not change the strength of the soft interaction but reduces x of the parton. Hence, one can deduce an evolution equation for $P_i(\sigma, x)$ expressing $P_i(\sigma, x)$ at the large scale Q^2 through $P_i(\sigma, x)$ at the input Q_0^2 scale ($i = q, \bar{q}, g$). For $x \geq 0.2$, where we expect a significant dependence of $P_{q(g)}(\sigma, x, Q_0^2)$ on x, perturbative QCD (pQCD) evolution leads to a decrease of $\sigma(x, Q^2)$ with an increase of Q^2. This is because the account of the QCD radiation—Q^2 evolution—shows that partons with given x and large Q^2 originate from larger x at the nonperturbative scale Q_0^2. As we argued above, for large x, the size of configuration is likely to decrease with an increase of x. Hence, the increase of p_t of the trigger for fixed x should lead to a gradual decrease of the average σ for the dominant configurations. In addition, in the gluon channel, one also expects a significant mixing between the contributions of (anti) quarks and gluons at Q_0^2.

To illustrate these effects, we used the Dokshitzer–Gribov–Lipatov–Altarelli–Parisi (DGLAP) evolution equations to evaluate the contributions of quark and gluon PDFs at $Q_0^2 = 4$ GeV^2 to the quark and gluon PDFs at $Q^2 = 10^4$ GeV^2. The results of this analysis are presented in Fig. 8 as fractions of the parton distribution (the left panel is for the u-quark PDF and the right panel is for the gluon PDF) at given x ($x = 0.1$, 0.3, and 0.5) and $Q^2 = 10^4$ GeV^2, which originate from the quark (solid curves) and gluon (dotted curves) PDFs at the input scale $Q_0^2 = 4$ GeV^2, which have the support on the $[x, x_{\rm cut}]$ interval. The plotted fractions are shown as functions of the cut-off parameter $x_{\rm cut}$, $x_{\rm cut} > x$. Thus, by construction, the shown fractions vanish in the $x_{\rm cut} \to x$ limit and rapidly tend to unity in the $x_{\rm cut} \to 1$ limit. Varying the parameter $x_{\rm cut}$ we examine the weight of different intervals of the light-cone variable x' at the input scale of the DGLAP evolution in the resulting quark and gluon PDFs at the higher scale Q^2. Such an analysis allows one to quantitatively study the effective trajectory of QCD evolution. (For an analysis of QCD evolution trajectories at small x, see [33]).

One can see from the figure that (i) $x_{\rm cut}$ is noticeably larger than x which means that the PDFs at high Q^2 originate from the broad $[x, x_{\rm cut}]$ interval at the input scale, and (ii) the gluon PDF receives a significant though not dominant contribution also from quarks at the initial scale. This

effect is somewhat smaller for lower Q^2. In summary, Fig. 8 illustrates that perturbative QCD evolution induces fluctuations in σ even if there is no dispersion at the initial scale.

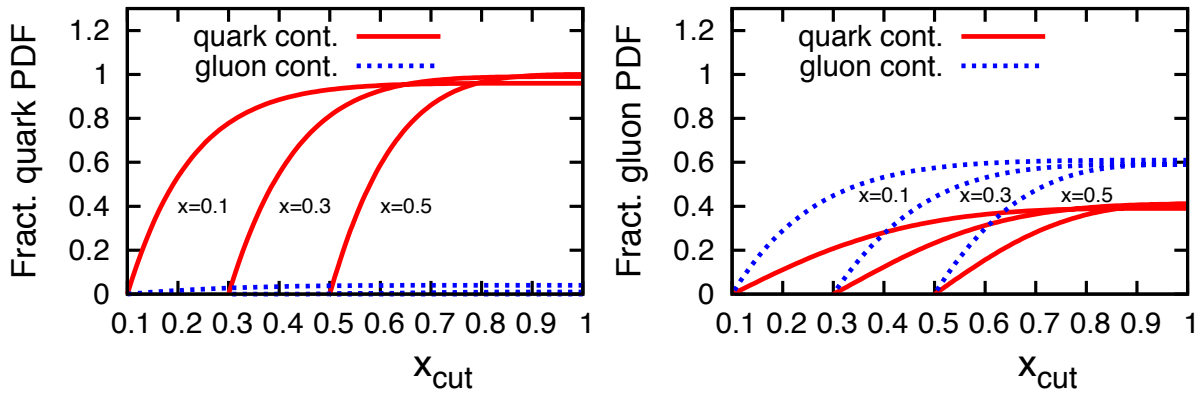

FIG. 8: Fractional contributions to the quark (left panel) and gluon (right panel) PDFs at $x = 0.1$, 0.3, and 0.5 and $Q^2 = 10^4$ GeV^2 originating from the interval $[x, x_{\rm cut}]$ at the input scale $Q_0^2 = 4$ GeV^2. The solid curves correspond to the quark contribution and the dotted curves are for the gluon contribution.

VI. FLUCTUATIONS AND CONDITIONAL PARTON DISTRIBUTIONS

In the previous sections we made a simplifying approximation that nuclear PDFs are the sums of nucleon PDFs. Deviations from this approximation are observed at $x \geq 0.4$ (the EMC effect) and small x. In the long run it would be possible to use the discussed processes to also study novel aspects of the nucleus partonic structure since they select nuclear configurations where many more nucleons are located in the cylinder around the transverse position of the hard interaction than on average. These high density nuclear configurations should have the different parton structure for at least for two reasons: (i) the leading twist nuclear shadowing should increase with a decrease of x due to an increase of the nucleon density in the cylinder of target nucleons interacting with the projectile at a fixed impact parameter as progressively more nucleons screen each other; (ii) the decrease of average internucleon distances within the cylinder should increase the modification of large-x parton distributions, i.e., the EMC effect, which is roughly proportional to the probability of the short range correlations in nuclei [20, 34].

A. Leading twist nuclear shadowing effect

In Sect. III we calculated the dependence of the nuclear gluon density (treated as a sum of the nucleon gluon densities) encountered by the projectile parton as a function of N_{coll}. We have demonstrated that the pattern strongly depends on the strength of fluctuations: if the fluctuations are neglected, the density is to a very good approximation given by $N_{coll}\, g_N(x,Q^2)$. At the same time, fluctuations slow down the increase of the gluon distribution by the factor of R_{HT} presented in Fig. 4.

Qualitatively we expect that with an increase of N_{coll}, nuclear shadowing for small $x_A < 0.01$ and antishadowing for $x_A \sim 0.1$ will increase. In the following, we will use the theory of leading twist nuclear shadowing, see the review in [33], to calculate the shadowing and compensating antishadowing effects. We restrict ourself to the limit when x_p of the parton of the proton is small enough (≤ 0.2) so that we can use $P_N(\sigma)$.

As a reference point, we consider the ratio of nuclear PDFs at the zero impact parameter $g_A(x,Q^2,b=0)$ and the properly normalized nucleon gluon density:

$$\frac{g_A(x,Q^2,b=0)}{T_A(b=0)g_N(x,Q^2)}\,, \tag{24}$$

which was calculated in Section 5.5 of [33].

The effective transverse gluon density probed by the projectile is:

$$g_A(x,Q^2,N_{coll}) = \frac{N_{coll}R_{HT}(N_{coll})}{N_{coll}(b=0)R_{HT}(N_{coll}(b=0))}g_A(x,Q^2,b=0)\,. \tag{25}$$

Defining now the ratio of the effective gluon densities for N_{coll} as

$$k = \frac{N_{coll}R_{HT}(N_{coll})}{N_{coll}(b=0)R_{HT}(N_{coll}(b=0))}\,, \tag{26}$$

we can calculate the shadowing and antishadowing effects—to a good approximation—by rescaling the nuclear density in the equations determining the shadowing effect by the factor of k. Using the results of Sec. II, we find $\langle N_{coll}\rangle \approx 14.5$ and from the inspection of Fig. 4 one can see that k can reach for large N_{coll} the values of up to $k=2$.

Figure 9 presents our predictions for the super ratio of $(g_A(x,Q^2,N_{coll})/g_A(x,Q^2))/g_A(x=0.2,Q^2,N_{coll})/g_A(x=0.2,Q^2))$ as a function of x for three values of $Q^2 = 4$, 10, and 10^4 GeV^2 and four values of $k = 0.5$, 1., 1.5, and 2. The shaded bands represent the theoretical uncertainty of the leading twist theory of nuclear shadowing associated with modeling of multiple (three and more) interactions of a hard probe with a nucleus [33]. One can see from the figure that the expected

modifications of nuclear conditional PDFs should be rather large, if one could use a hard probe with a moderate virtuality of, e.g., 100 GeV^2. For the case of dijets with $p_t \geq 100$ GeV/c, the effect is rather small for a wide range of x and represents a small correction for the studies of the effects of selection of large x_p in the currently studied processes with a dijet trigger.

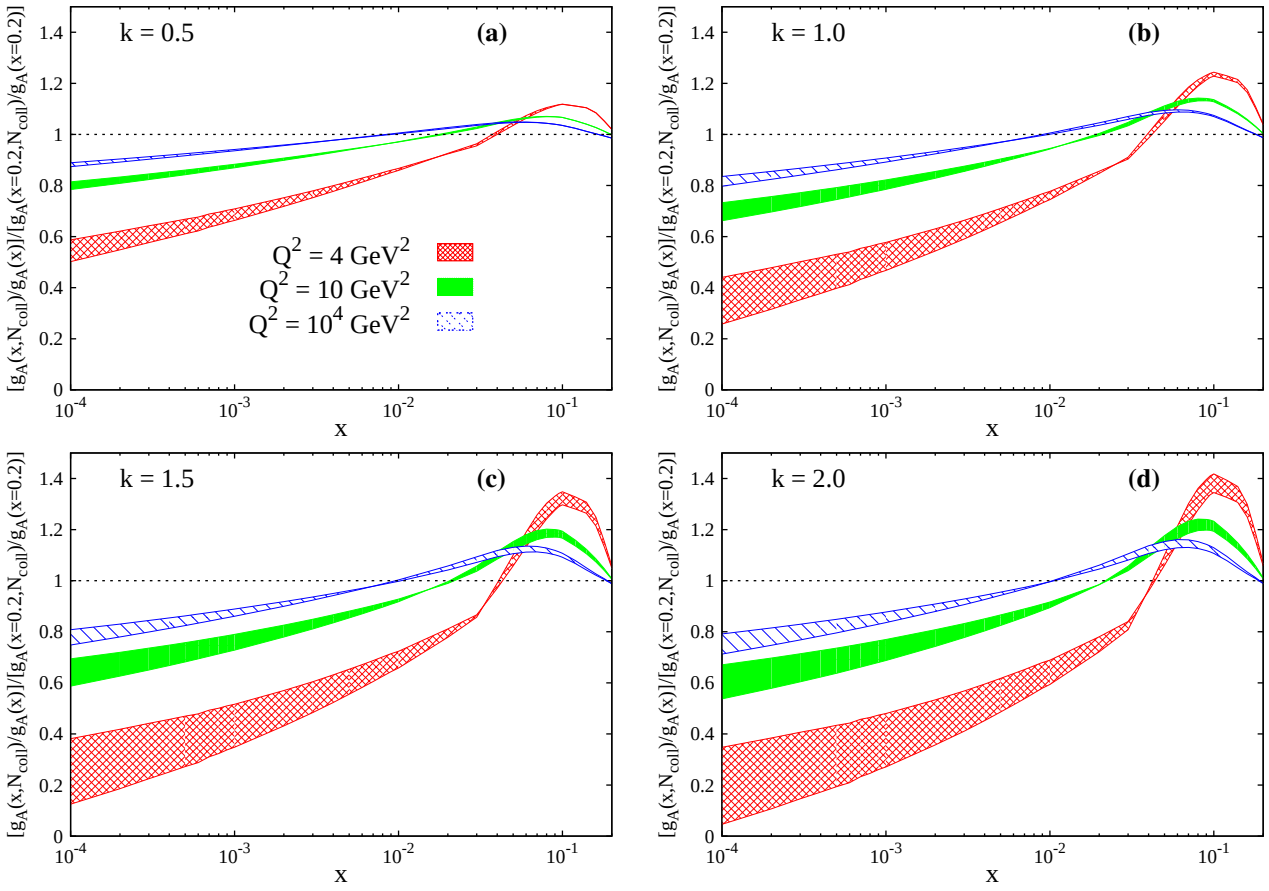

FIG. 9: Ratio of the nuclear gluon conditional distribution for given N_{coll} and the inclusive gluon density normalized to their values at $x = 0.2$ as a function of x for different values of Q^2 and k. See text for details.

Note here that due to uncertainties in the procedure for determination of N_{coll}, the optimal procedure would be to consider the ratios of cross sections for small x_A and $x_A \sim 0.2$, where nuclear effects are negligibly small, for the same N_{coll} and to preferably use the same range of x_p.

The average N_{coll} for the top 1% of collisions can be estimated using the results presented in Fig. 1. We find for these collisions that $\langle N_{coll} \rangle \sim 20(25)$ for $\omega_\sigma = 0(0.1)$ and, hence, $k \sim 1.5$ (1.25), which corresponds to quite a significant deviation from the x dependence of inclusive nuclear PDFs.

The quark channel analogue of Fig. 9, Fig. 10 shows our predictions for the superratio $(\bar{u}_A(x, Q^2, N_{coll})/\bar{u}_A(x, Q^2))/\bar{u}_A(x = 0.2, Q^2, N_{coll})/\bar{u}_A(x = 0.2, Q^2))$ for the $\bar{u}_A$ quark.

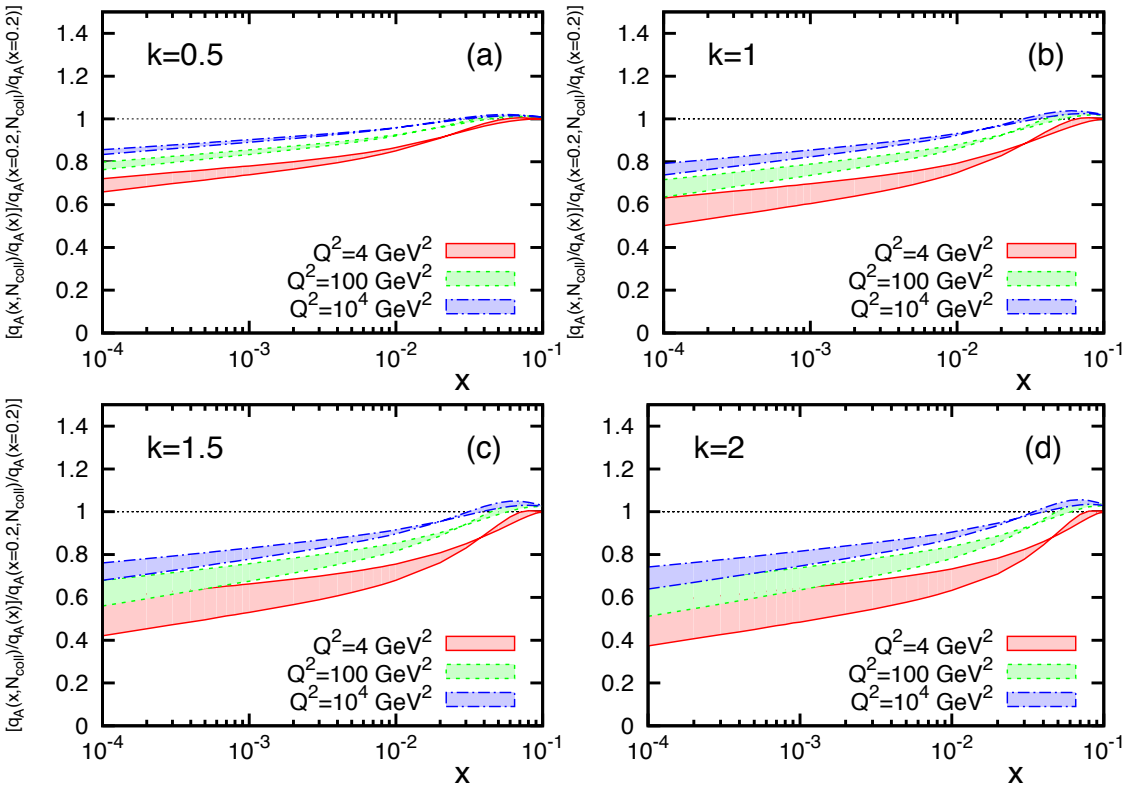

FIG. 10: The $\bar{u}_A$ quark superratio $(\bar{u}_A(x,Q^2,N_{coll})/\bar{u}_A(x,Q^2))/\bar{u}_A(x=0.2,Q^2,N_{coll})/\bar{u}_A(x=0.2,Q^2))$ as a function of x for different values of Q^2 and k. See Fig. 9 for comparison and text for details.

B. The $x_A \sim 0.5$ region

The above calculation demonstrates that the distances between nucleons in nuclei are reduced for large-N_{coll} triggers. This should have implications for the large-x_A conditional PDFs of the nucleus. Indeed it is known that nuclear PDFs at large x_A are significantly suppressed as compared to the free nucleon ones for x between 0.5 and 0.7 and large Q^2. The scale of the suppression for heavy nuclei and large Q^2 is on the scale of 20% as measured at CERN in the kinematics where the leading twist definitely dominates, see the review [35].

It is natural to expect that the EMC effect originates due to pairs of nucleons coming close together and deforming each other wave functions. Higher the nucleon momentum, further it is off-mass-shell, and, hence, larger the effect is. Hence one can expect that the EMC effect is mostly due to the presence of short-range correlations [20]. The recent analyses of the data are consistent with this expectation, see the review and references in [34].

For heavy nuclei, the probability of short-range correlations (SRCs) is approximately proportional to the local nuclear density. Hence, one can estimate the magnitude of the modification of

nuclear PDFs due to selection of the large-N_{coll} events as

$$\frac{(1-f_A/f_N)_{N_{coll}}}{1-f_A/f_N} \sim k\,, \tag{27}$$

where f_A and f_N denote the quark nucleus and nucleon densities, respectively. Since $k \sim 1.3-1.5$ for the 1% of events with the highest N_{coll}, the expected change of the EMC effect is rather modest. Still this selection appears to provide a unique opportunity to probe nuclear matter at the density significantly higher than the average one.

A more accurate analysis should take into account the dominance of pn correlations, see review in [36, 37], the interplay between attraction and repulsion in SRCs, etc. Such an analysis will be presented elsewhere.

VII. SUGGESTIONS FOR FUTURE ANALYSES

In the future analyses of the data it would be important to study jet production as a function of centrality for bins of x_p and x_A to separate possible effects of the conditional nuclear PDFs and effects of color fluctuations. Testing that different processes with the same x_p show the same centrality pattern is critical.

It would be also interesting to study the effect at fixed x_p as a function of p_t of the jet. Such a dependence arises due to DGLAP evolution since σ for a configuration depends on the "parent" x_p at the low Q^2 scale, which is larger than x_p for the jet (Fig. 8).

Studies of fluctuation effects for $P_g(x,Q^2)$ in the gluon channel will be challenging as the deviations from average due to squeezing are expected for $x > 0.2-0.3$ at the input scale Q_0^2 corresponding to somewhat smaller x for jets with $p_T \sim 100$ GeV (Fig. 8). Still the crossover point between the gluon and quark contributions for such p_T is $x \sim 0.2$ so that in view of the significant quark contribution to $g_N(x,Q^2)$, the effect of the smaller average gluon $\sigma_g(x,Q_0^2)$ would be rather small — on the scale of 30%. Hence one would need to use the processes where the gluon contribution is enhanced, for example, production of heavy quarks at relatively modest p_t, which is obviously experimentally challenging. Nevertheless it would be highly desirable to study CF effects separately for quarks and gluons since the squeezing is likely to be different and starts in the gluon case at smaller x.

If one would observe a pattern similar to the one for generic jets, it would strongly suggest presence of the EMC effect for gluons due to suppression of weakly interacting contributions in bound nucleons [20].

One should also look for kinematics of small x_p where the contribution of configurations with σ larger than average should be enhanced.

Measurements using $W^{\pm}$ can be used to study the difference of the interaction strength of configurations with leading u- and d-quarks. An advantage of this process which maybe possible to study at RHIC in the forward kinematics is that any effects related to energy–momentum conservation cancel out in the ratio of the cross sections at same x.

VIII. CONCLUSIONS

In conclusion, we have demonstrated that it is possible to use the LHC pA data to understand the correlation between the parton distribution in the nucleon and its interaction strength and to explore fine details of the nuclear parton structure in the EMC effect and nuclear shadowing regions.

The authors thank members of the ALICE, ATLAS and CMS collaborations and especially B. Cole, D. C. Gulhan, Y.-J. Lee, and J. Schukraft for useful discussions. M. Strikman's research was supported by the U.S. Department of Energy Office of Science, Office of Nuclear Physics under Award Number DE-FG02-93ER40771. L. Frankfurt research was supported by BSF grant.

Appendix A: On the account of the momentum conservation in the color fluctuation approach

Conservation of momentum implies that the proton momentum in proton–nucleus inelastic collisions is split among several collisions. Hence, the energy released in one inelastic pN collision is a decreasing function of the number of collisions and it is necessity to take this effect into account. The aim of this appendix is to explain that energy–momentum conservation is effectively taken into account in the color fluctuation (CF) formulae for the total cross sections, the number of wounded nucleons, etc. In contrast, the celebrated Abramovsky–Gribov–Kancheli (AGK) cancelation [6] among shadowing contributions for the single inclusive spectrum including inelastic processes due to the cut of $N \geq 2$ ladders for central rapidities is violated and the resulting formulae contain the additional factor $R_{N_{coll}}$ which cannot be evaluated at present in a model-independent way, see Eq. (A2). The explanation of above statements involves several steps which are outlined below.

In QCD, longitudinal distances comparable to the atomic scale dominate in pA collisions at the LHC (to simplify the discussion, we work in the nucleus rest frame). Indeed it follows from the

uncertainty principle that the lifetime of a fast proton with the momentum P_N and the energy E in the configuration $|n\rangle$ is:

$$t_{coh} = \frac{1}{(E_n - E)} = \frac{2P_N}{\sum_i \frac{m_i^2 + p_{i\,t}^2}{x_i} - m_p^2}\,, \tag{A1}$$

where m_i, x_i, and $p_{i\,t}$ are the masses of constituents, their light-cone fractions and transverse momenta, respectively. Hence, during the passage through the nucleus and far behind it, the transverse positions of the fast constituents of the projectile do not change. These constituents interact with a target through ladders attached to these constituents. This interaction may destroy coherence of these constituents with spectator constituents leading to multi-hadron production.

It follows from Eq. (A1) that the proton energy is divided among fast partons long before the collision. So the energy–momentum conservation is explicitly satisfied for the interaction of partons with a target. On the contrary, in the Glauber picture, the projectile nucleon is destroyed in the first collision and combines back into the nucleon during the time between collisions with different nucleons of the nucleus. This is obviously impossible at high energies since such a transition takes too long a time $\approx t_{coh}$. Another problem is that due to energy–momentum conservation, a significant part of the projectile energy is already lost in the first inelastic collision diminishing the phase volume for other inelastic collisions. The Glauber model derived within quantum mechanics ignores energy–momentum conservation which is controversial when $N \geq 2$ ladders are cut. These puzzles are naturally resolved in QCD since the contribution of the planar Feynman diagrams relevant for the Glauber model disappears at high energies where processes with hadron production dominate. The complete cancellation of the planar diagrams has been demonstrated for high energy processes by direct calculations of the relevant Feynman diagrams in Refs. [8, 9] using analytic properties of amplitudes in the plane of masses of diffractively produced states.

Gribov suggested to decompose the contribution of non-planar diagrams over the sum of the pole corresponding to the initial hadron and inelastic diffractive states. Exploring both representations—kind of duality between quark–gluon and hadron degrees of freedom—allows one to analyze implications of the energy–momentum conservation. In practice the derived formulae for nuclear shadowing differ from the formulae of the Glauber approximation by the small inelastic shadowing correction [5]. This pre-QCD approach leads to the following models : (i) the Gribov–Glauber model, which includes inelastic diffractive processes in the intermediate states, and (ii) the color fluctuation approach [2, 3], which takes into account the fluctuations of the interaction strength in the form familiar from the properties of bound states in QCD.

The color fluctuation approach [2] is a generalization of the pre-QCD assumption of Good and

Walker [11] that one can present the high energy hadron–nucleus interaction as a superposition of interactions of the initial hadron in the configurations of different strengths which do not change during the propagation through the nucleus. The CF approach includes low-mass fluctuations as well as the fluctuations into large diffractive masses. The natural pattern for the contribution of large diffractive masses is the triple Pomeron mechanism which takes into account that the intermediate masses increase with energy. This mechanism allows for the splitting of energy in the interaction with several nucleons to occur at rapidities rather far away from the nucleon's rapidity providing a mechanism for production of leading nucleons in the interactions of the proton with several nucleons.

In the case of the hadron interaction with two nucleons, the shadowing correction to the total cross section is expressed through the cross section of diffraction (elastic plus inelastic) [5]. This Gribov formula follows also from the Abramovsky–Gribov–Kancheli combinatorics for cross sections [6]. It follows also from the model [38], which includes fluctuations of the interaction strength in the form of the Miettinen–Pumplin relation [Eq. (3)]. The Gribov formula for shadowing in proton - deuteron scattering includes the triple Pomeron contribution exactly and allows one to express the shadowing contribution to $\sigma_{tot}(pd)$ through the diffractive cut of the Feynman diagrams with exchange by two ladders. So for the interaction with two nucleons, energy–momentum conservation is accurately taken into account. Higher moments are also expressed through experimental observable, see the determination of $\left\langle \sigma^3 \right\rangle$ in [2].

Thus, all factors related to the increase of the cross section with energy are included into $P(\sigma)$. No additional factors in the CF formulae are required to describe also the number of wounded nucleons since it is evaluated through the multiplicity of hadrons in the kinematics close to the nucleus fragmentation region [1]. In this kinematics hadron multiplicity is a slow function of s as the consequence of the Feynman scaling.

For hadron multiplicity in the center of rapidity and in the proton fragmentation region, the answer is more complicated. Note here that the hadron inclusive cross section at central rapidities in pp interaction grows with energy approximately as $(s/s_0)^\kappa$, where $\kappa \sim 0.25$. Thus, the hadron inclusive cross section for the pN interaction contains the factor of $(x_i s/s_0)^\kappa$ instead of $(s/s_0)^\kappa$ within the Gribov–Glauber model and the CF approach, where x_i is the fraction of the projectile momentum carried by the interacting parton "i" or a group of partons. The factor $(x_i)^\kappa$ is not included in $P(\sigma)$ since it is additional to the CF series in terms of $\langle \sigma^n \rangle$ defining $P(\sigma)$. Hence, it follows from energy–momentum conservation that the hadron inclusive cross section due to the processes where $N > 1$ ladders are cut is suppressed by the factor of R_N as compared to the

formulae of the Gribov–Glauber approximation and the CF approach combined with the AGK cutting rules:

$$R_N = \frac{\sum_n \int d\tau_n \left|\psi_n(x_1,...x_N,...x_n)\right|^2 (1/N) \sum_{i=1}^{i=N} (x_i)^\kappa}{\sum_m \int d\tau_m (x_i)^\kappa \left|\psi_m(x_1,...x_N,...x_m)\right|^2} \,. \tag{A2}$$

where $d\tau_n = (dx_i/x_i..dx_N/x_N...dx_n/x_n)\delta(\sum_i x_i - 1)$ is the phase volume ; $n \geq N$ is the number of finite-x partons in a given configuration. R_N would be equal to unity in the case of identical ladders originating from the partons with approximately equal x_i. If N is large, R_N becomes significantly smaller than unity due to tighter phase volume restrictions in the numerator than in the denominator and due to a decrease of the average energy allowed for inelastic collisions. The deviation of R_N from unity violates AGK combinatorics.

Within the discussed picture, energy-momentum conservation for the final state is realized through a reduction of the number of fast spectator constituents in the nucleon with an increase of the number of wounded nucleons leading to the strong suppression of production of hadrons in the nucleon fragmentation region and close to the central region for large N_{coll}. In the discussion above, we neglected the contribution of hard interactions into the bulk structure of the events. This may be an oversimplification for the LHC energies, where the interaction of hard partons with large x_p may become black up to the virtualities of few GeV for central collisions. This would lead to further suppression of the leading hadron production, p_t broadening of the forward spectrum and an additional flow of energy to the central rapidities.

[1] ATLAS Conference note: ATLAS-CONF-2013-096.

[2] H. Heiselberg, G. Baym, B. Blaettel, L. L. Frankfurt and M. Strikman, Phys. Rev. Lett. **67**, 2946 (1991); Phys. Rev. C **52**, 1604 (1995)

[3] M. Alvioli and M. Strikman, Phys. Lett. B **722**, 347 (2013)

[4] D. Dutta, K. Hafidi and M. Strikman, Prog. Part. Nucl. Phys. **69**, 1 (2013) [arXiv:1211.2826 [nucl-th]].

[5] V. N. Gribov, Sov. Phys. JETP **29** (1969) 483 [Zh. Eksp. Teor. Fiz. **56** (1969) 892].

[6] V. A. Abramovsky, V. N. Gribov and O. V. Kancheli, Yad. Fiz. **18** (1973) 595 [Sov. J. Nucl. Phys. **18** (1974) 308].

[7] L. Frankfurt, V. Guzey and M. Strikman, J. Phys. G **27**, R23 (2001)

[8] S. Mandelstam, Nuovo Cim. **30** (1963) 1148.

[9] V. N. Gribov, Sov. Phys. JETP **26** (1968) 414 [Zh. Eksp. Teor. Fiz. **53** (1967) 654].

[10] H. I. Miettinen and J. Pumplin, Phys. Rev. D **18**, 1696 (1978).

[11] M. L. Good and W. D. Walker, Phys. Rev. **120** (1960) 1857.

[12] B. Blaettel, G. Baym, L. L. Frankfurt and M. Strikman, Phys. Rev. Lett. **70**, 896 (1993); Phys. Rev. D **47**, 2761 (1993).

[13] K. Goulianos, private communication.

[14] F. E. Low, Phys. Rev. D **12**, 163 (1975).

[15] C. E. Coleman-Smith and B. Müller, Phys. Rev. D **89**, 025019 (2014)

[16] L. Bertocchi and D. Treleani, J. Phys. G G **3** (1977) 147.

[17] V. Guzey and M. Strikman, Phys. Lett. B **633**, 245 (2006); Phys. Lett. B **663**, 456 (2008).

[18] M. Alvioli, H. -J. Drescher and M. Strikman, Phys. Lett. B **680**, 225 (2009)

[19] L. Frankfurt, M. Strikman, D. Treleani and C. Weiss, Phys. Rev. Lett. **101**, 202003 (2008) [arXiv:0808.0182 [hep-ph]].

[20] L. L. Frankfurt and M. I. Strikman, Nucl. Phys. B **250** (1985) 143.

[21] L. Frankfurt, M. Strikman and C. Weiss, Phys. Rev. D **69**, 114010 (2004)

[22] L. Frankfurt and M. Strikman, Phys. Rev. D **66**, 031502 (2002)

[23] L. Frankfurt, M. Strikman and C. Weiss, Phys. Rev. D **83** (2011) 054012

[24] J. Jia, Phys. Lett. B **681**, 320 (2009)

[25] M. Diehl and P. Kroll, Eur. Phys. J. C **73**, 2397 (2013) [arXiv:1302.4604 [hep-ph]].

[26] ATLAS Conference note: ATLAS-CONF-2013-105.

[27] S. Chatrchyan *et al.* [CMS Collaboration], arXiv:1401.4433 [nucl-ex].

[28] B. Abelev *et al.* [ALICE Collaboration], Phys. Lett. B **712** (2012) 165

[29] R. Bala [for the ALICE Collaboration], arXiv:1309.6570 [nucl-ex]

[30] M. Strikman, Phys. Rev. D **84** (2011) 011501

[31] M. Y. Azarkin, I. M. Dremin and M. Strikman, arXiv:1401.1973 [hep-ph].

[32] L. Frankfurt, M. Strikman and C. Weiss, Annalen Phys. **13**, 665 (2004)

[33] L. Frankfurt, V. Guzey and M. Strikman, Phys. Rept. **512**, 255 (2012)

[34] O. Hen, D. W. Higinbotham, G. A. Miller, E. Piasetzky and L. B. Weinstein, Int. J. Mod. Phys. E **22**, 1330017 (2013)

[35] M. Arneodo, Phys. Rept. **240**, 301 (1994).

[36] L. Frankfurt, M. Sargsian and M. Strikman, Int. J. Mod. Phys. A **23**, 2991 (2008)

[37] M. Alvioli, C. Ciofi degli Atti, L. P. Kaptari, C. B. Mezzetti and H. Morita, Int. J. Mod. Phys. E **22**, 1330021 (2013)

[38] B. Z. Kopeliovich and L. I. Lapidus, Pisma Zh. Eksp. Teor. Fiz. **28** (1978) 664.

[39] In contrast, in pp collisions, fluctuations of the impact parameter dominate in a wide kinematic range. For example, the strong positive correlation between the hadron multiplicity, N_h, and the rate of production of J/ψ, D, and B mesons observed by ALICE [28, 29] appears to be dominated by selection of different b up to $N_h/\langle N_h\rangle \sim 3$ [30]. The same pattern in the CMS data was recently demonstrated for high p_t jet production [31].

[40] Importance of small-size configurations at large x_p could also be studied in hard diffraction at the LHC

by studying hard diffraction at fixed $x_{I\!P}$ and fixed β (the fraction of the energy carried by the parton belonging to the diffracting proton) as a function of x_p. The gap survival probability should increase when $x_p \geq 0.5$.